T H E   A R C H I V E   O F   M E C H A N I C A L   E N G I N E E R I N G

MIGUEL A. NAYA*, JAVIER CUADRADO*, DANIEL DOPICO*, URBANO LUGRIS*

AN EFFICIENT UNIFIED METHOD FOR THE COMBINED SIMULATION OF MULTIBODY AND HYDRAULIC DYNAMICS: COMPARISON WITH SIMPLIFIED AND CO-INTEGRATION APPROACHES

A formulation developed at the Laboratory of Mechanical Engineering allows robust and efficient simulation of large and complex multibody systems. Simulators of cars, excavators and other systems have been developed showing that real-time simulations are possible even when facing demanding manoeuvres.

Hydraulic actuators are present in many industrial applications of multibody systems, like in the case of the heavy machinery field. When simulating the dynamics of this kind of problems that combine multibody dynamics and hydraulics, two different approaches are common: to resort to kinematically guide the variable length of the actuator, thus avoiding the need to consider the dynamics of the hydraulic system; or to perform a multi-rate integration of both subsystems if a more detailed description of the problem is required, for example, when the objective of the study is to optimize the pump control.

This work addresses the inclusion of hydraulic actuators dynamics in the above-mentioned self-developed multibody formulation, thus leading to a unified approach. An academic example serves to compare the efficiency, accuracy and ease of implementation of the simplified (kinematic guidance), multi-rate and unified approaches. Such a comparison is the main contribution of the paper, as it may serve to provide guidelines on which approach to select depending on the problem characteristics.

1. Introduction

Several years ago, the authors proposed a method for the efficient simulation of the dynamics of multibody systems [1]: the modeling of the system was carried out in natural or fully-Cartesian coordinates, the equations of motion were stated as an index-3 augmented Lagrangian formulation,

---

* *Laboratory of Mechanical Engineering, University of La Coruña, Ferrol, 15403, Spain; e-mail: minaya@cdfudces*

the numerical integration was performed through Newmark-type algorithms, and the resulting velocities and accelerations were projected into their corresponding constraint manifolds. The formalism showed to be robust and efficient: it worked properly in mechanisms with singular configurations or changing topologies, and provided successful results for large and complex industrial problems, like the detailed models of cars and excavators, allowing integration time steps as large as 10 ms. Some years later, the method was extended [2] so as to consider the modeling in joint coordinates (dependent and relative coordinates), taking advantage of the recursive kinematics and dynamics allowed for such an approach, which led to a method with improved efficiency for large systems.
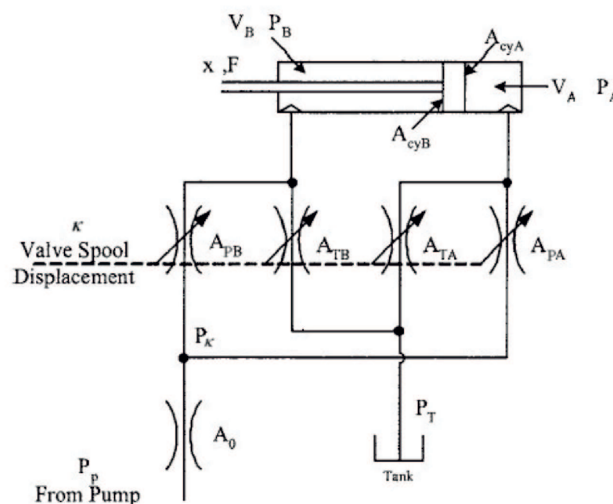

Fig. 1. Diagram of a hydraulic cylinder and valve

Hydraulic actuators play a relevant role in many industrial fields, like for example in most heavy machinery systems [3, 4]. The dynamics of such devices are usually modeled in terms of the orifice equations, volumes and pressure areas, as depicted in Fig. 1. Pressure rates for the volumes on both sides of the cylinder piston are derived from fluid continuity and compressibility considerations [5] as

$$\dot{p}_A = \frac{\beta_A}{V_A} \left(-\dot{V}_A + Q_{PA} + Q_{TA} + Q_{BA} \right) \tag{1}$$

$$\dot{p}_B = \frac{\beta_B}{V_B} \left(-\dot{V}_B + Q_{PB} + Q_{TB} + Q_{BA} \right) \tag{2}$$

where V_A and V_B are the volumes at each side of the cylinder and $\dot{V}_A$, $\dot{V}_B$ are their speeds of variation. Q_{PA}, Q_{PB} represent the flow incoming to chamber

A or B from the pump, Q_{TA}, Q_{TB} are the flows to the tank from chamber A or B, while Q_{BA} constitutes the leakage flow and is commonly neglected. The bulk modulus at each side of the cylinder, β_i, is obtained as a function of the pressures as

$$\beta_i = \frac{1 + ap_i + bp_i^2}{a + 2bp_i} \tag{3}$$

with a and b being known constants for the fluid. The flow across each orifice area, A_{orf}, in a hydraulic valve is given by

$$Q = A_{orf} C_d \sqrt{\frac{2(p_{in} - p_{out})}{\rho}} sign(p_{in} - p_{out}) \tag{4}$$

where p_{in} and p_{out} are the pressures at both sides of the orifice and C_d is the flow discharge coefficient for a sharp orifice opening area.

In the valve, there are four orifice areas which are a nonlinear function of the spool displacement, κ, corresponding to $A_{PA}(\kappa)$, $A_{TA}(\kappa)$, $A_{PB}(\kappa)$, $A_{TB}(\kappa)$. The displacement of the spool includes some dead zones to minimize leakage [6]. The variation of the pressure provided by the pump is a nonlinear function of the speed, the flow, the leakages and the geometry of the pump, but this is not taken into account in this work.

A common simplified technique to include the behavior of hydraulic actuators within simulations of multibody dynamics consists of kinematically guiding the variable length corresponding to the distance between the ends of the hydraulic actuator [7]. The guidance law, which provides the actuator length as function of the driving inputs (provided, for instance, by the machine operator), may be just a linear mapping, or may account for force or speed limitations and other characteristics of the real power system.

However, for some applications, e.g. when optimization of the pump control is sought, a more detailed modeling is required, and the dynamics of hydraulic actuators should be taken into account. Some attempts have been presented in the literature in this direction [8, 9]. From the integration point of view, two different approaches have been followed, namely, the unified approach, and the co-integration.

The first one combines the hydraulic and multibody equations, thus yielding a single system [10, 11] that is then integrated in time.

In the second approach, one problem leads the solution process and, usually, its integration time-step size is larger. Therefore, both problems are integrated separately, but information is exchanged between them at every integration time step of the main process. This is known as multi-rate integration, and can be carried out by either employing a different software for each problem (co-simulation) [9, 12] or a single environment where both

problems are integrated separately (co-integration) [13,14]. Hydraulic devices are easily modeled by a few first-order nonlinear differential equations, but it is a numerically stiff set of equations due to the high "stiffness" of the hydraulic fluid, which is characterized by a bulk modulus that may raise to 700 MPa. This problem may be overcome by using a very small time-step size for the integration that ranges, typically between 10^{-6} s and 10^{-4} s [15]. Consequently, the multibody integration leads the process, and the hydraulic problem is solved with a smaller time-step size.

In this work, the first approach from those that take the hydraulic dynamics into account is addressed: both hydraulic and multibody dynamic equations are combined within the formalism mentioned at the beginning of the Section in a unified approach. The efficiency of this scheme is tested by comparison with the kinematic guidance of hydraulic actuators. The accuracy of the solution is contrasted with that of a co-integration scheme. The comparison of the three approaches may be considered as the main contribution of the paper, as it aims to provide guidelines that help to find out which is the most suitable approach depending on the problem characteristics.

The organization of the paper is as follows: the original method for multibody dynamics is briefly exposed in Section 2; the inclusion of the hydraulic dynamic equations is addressed in Section 3, and the resulting formalism is obtained; an academic example aimed to test the behavior of the proposed scheme is presented in Section 4, while in Section 5 the results coming from the simulation of the example are discussed and compared with those of the other approaches mentioned above; finally, the conclusions are summarized in Section 6.

2. The original multibody method

The original method for the dynamics of multibody systems is described in [1], but a brief overview is presented in this Section. The modeling is carried out in dependent fully-Cartesian coordinates, also known as natural coordinates. Further explanation about these coordinates and the constraints they lead to can be found in [16].

The equations of motion of the whole multibody system are given by an index-3 augmented Lagrangian formulation in the form

$$\mathbf{M\ddot{q}} + \mathbf{\Phi_q}^T \alpha \mathbf{\Phi} + \mathbf{\Phi_q}^T \boldsymbol{\lambda}^* = \mathbf{Q} \tag{5}$$

where $\mathbf{M}$ is the mass matrix, $\mathbf{\ddot{q}}$ the accelerations vector, $\mathbf{\Phi_q}$ the Jacobian matrix of the constraint equations, α the penalty factor, $\mathbf{\Phi}$ the constraints vector, $\boldsymbol{\lambda}^*$ the Lagrange multipliers and $\mathbf{Q}$ the vector of applied and velocity dependent inertia forces. The Lagrange multipliers are obtained from the

following iteration process (given by sub-index i, while sub-index n stands for the time step),

$$\boldsymbol{\lambda}_{i+1}^* = \boldsymbol{\lambda}_i^* + \alpha \boldsymbol{\Phi}_{i+1} \quad i = 0, 1, 2, ... \tag{6}$$

where the value of $\boldsymbol{\lambda}_o^*$ is taken equal to the $\boldsymbol{\lambda}^*$ obtained in the previous time step.

As integration scheme, the implicit single-step trapezoidal rule is adopted. The corresponding difference equations in velocities and accelerations are:

$$\dot{\mathbf{q}}_{n+1} = \frac{2}{\Delta t} \mathbf{q}_{n+1} + \hat{\dot{\mathbf{q}}}_n$$

$$\ddot{\mathbf{q}}_{n+1} = \frac{4}{\Delta t^2} \mathbf{q}_{n+1} + \hat{\ddot{\mathbf{q}}}_n \tag{7}$$

with,

$$\hat{\dot{\mathbf{q}}}_n = - \left(\frac{2}{\Delta t} \mathbf{q}_n + \dot{\mathbf{q}}_n \right)$$

$$\hat{\ddot{\mathbf{q}}}_n = - \left(\frac{4}{\Delta t^2} \mathbf{q}_n + \frac{4}{\Delta t} \dot{\mathbf{q}}_n + \ddot{\mathbf{q}}_n \right) \tag{8}$$

Dynamic equilibrium can be established at time step $n+1$ by introducing the difference equations (6) and (7) into the equations of motion (4), leading to

$$\frac{4}{\Delta t^2} \mathbf{M} \mathbf{q}_{n+1} + \boldsymbol{\Phi}_{\mathbf{q}n+1}^T (\alpha \boldsymbol{\Phi}_{n+1} + \boldsymbol{\lambda}_{n+1}) - \mathbf{Q}_{n+1} + \mathbf{M} \hat{\ddot{\mathbf{q}}}_n = 0 \tag{9}$$

For numerical reasons, the scaling of Eq. (8) by a factor of $\Delta t^2/4$ seems to be advisable, thus yielding

$$\mathbf{M} \mathbf{q}_{n+1} + \frac{\Delta t^2}{4} \boldsymbol{\Phi}_{\mathbf{q}n+1}^T (\alpha \boldsymbol{\Phi}_{n+1} + \boldsymbol{\lambda}_{n+1}) - \frac{\Delta t^2}{4} \mathbf{Q}_{n+1} + \frac{\Delta t^2}{4} \mathbf{M} \hat{\ddot{\mathbf{q}}}_n = 0 \tag{10}$$

or, symbolically $\mathbf{f}(\mathbf{q}_{n+1}) = 0$.

In order to obtain the solution of this nonlinear system, the widely used iterative Newton-Raphson method is applied

$$\left[\frac{\partial \mathbf{f}(\mathbf{q})}{\partial \mathbf{q}} \right]_i \Delta \mathbf{q}_{i+1} = - [\mathbf{f}(\mathbf{q})]_i \tag{11}$$

being the residual vector,

$$[\mathbf{f}(\mathbf{q})] = \frac{\Delta t^2}{4} \left(\mathbf{M} \ddot{\mathbf{q}} + \boldsymbol{\Phi}_{\mathbf{q}}^T \alpha \boldsymbol{\Phi} + \boldsymbol{\Phi}_{\mathbf{q}}^T \boldsymbol{\lambda}^* - \mathbf{Q} \right) \tag{12}$$

and the approximated tangent matrix,

$$\left[\frac{\partial \mathbf{f}(\mathbf{q})}{\partial \mathbf{q}}\right] = \mathbf{M} + \frac{\Delta t}{2}\mathbf{C} + \frac{\Delta t^2}{4}\left(\mathbf{\Phi}_{\mathbf{q}}^T \alpha \mathbf{\Phi}_{\mathbf{q}} + \mathbf{K}\right) \tag{13}$$

where $\mathbf{C}$ and $\mathbf{K}$ represent the contribution of damping and elastic forces of the system provided they exist.

The procedure explained above yields a set of positions $\mathbf{q}_{n+1}$ that not only satisfies the equations of motion (5), but also the constraint conditions $\mathbf{\Phi} = 0$. However, it is not expected that the corresponding sets of velocities and accelerations satisfy $\dot{\mathbf{\Phi}} = 0$ and $\ddot{\mathbf{\Phi}} = 0$, because these conditions have not been imposed in the solution process. To overcome this difficulty, velocities and accelerations are projected into their corresponding constraint manifolds. The projection leading matrix is the same tangent matrix of Eq. (13). Therefore, triangularization is avoided and projections in velocities and accelerations are carried out with just forward reductions and back substitutions.

If $\dot{\mathbf{q}}^*$ and $\ddot{\mathbf{q}}^*$ are the velocities and accelerations obtained after convergence has been achieved within the Newton-Raphson iteration, their projected counterparts $\dot{\mathbf{q}}$ and $\ddot{\mathbf{q}}$ are calculated from

$$\left[\mathbf{W} + \frac{\Delta t^2}{4}\mathbf{\Phi}_{\mathbf{q}}^T \alpha \mathbf{\Phi}_{\mathbf{q}}\right]\dot{\mathbf{q}} = \mathbf{W}\dot{\mathbf{q}}^* - \frac{\Delta t^2}{4}\mathbf{\Phi}_{\mathbf{q}}^T \alpha \mathbf{\Phi}_t \tag{14}$$

for the velocities, and

$$\left[\mathbf{W} + \frac{\Delta t^2}{4}\mathbf{\Phi}_{\mathbf{q}}^T \alpha \mathbf{\Phi}_{\mathbf{q}}\right]\ddot{\mathbf{q}} = \mathbf{W}\ddot{\mathbf{q}}^* - \frac{\Delta t^2}{4}\mathbf{\Phi}_{\mathbf{q}}^T \alpha \left(\dot{\mathbf{\Phi}}_{\mathbf{q}}\dot{\mathbf{q}} + \dot{\mathbf{\Phi}}_t\right) \tag{15}$$

for the accelerations, being,

$$\mathbf{W} = \mathbf{M} + \frac{\Delta t}{2}\mathbf{C} + \frac{\Delta t^2}{4}\mathbf{K} \tag{16}$$

3. The proposed method for multibody and hydraulic dynamics

The method described in the previous Section is extended to also consider the hydraulic dynamic equations. The index-3 augmented Lagrangian formulation is incremented with the pressure variation equations, leading to the following combined system of equations:

$$\mathbf{M}\ddot{\mathbf{q}} + \mathbf{\Phi}_{\mathbf{q}}^T \alpha \mathbf{\Phi} + \mathbf{\Phi}_{\mathbf{q}}^T \lambda^* = \mathbf{Q}(\mathbf{q}, \dot{\mathbf{q}}, \mathbf{p})$$
$$\dot{\mathbf{p}} = \mathbf{h}(\mathbf{p}, \mathbf{q}, \dot{\mathbf{q}}) \tag{17}$$

where vector $\mathbf{p}$ contains the pressures of the chambers (two for each hydraulic cylinder). The dependency of both the applied forces vector $\mathbf{Q}$ and the function $\mathbf{h}$ with respect to positions $\mathbf{q}$, velocities $\dot{\mathbf{q}}$ and pressures $\mathbf{p}$ is considered to be known. The Lagrange multipliers are obtained from the same iteration process already described in the previous Section.

Again, the implicit single-step trapezoidal rule is adopted as integration scheme. The corresponding difference equations in velocities, accelerations and pressure derivatives are,

$$\dot{\mathbf{q}}_{n+1} = \frac{2}{\Delta t}\mathbf{q}_{n+1} + \hat{\dot{\mathbf{q}}}_n$$

$$\ddot{\mathbf{q}}_{n+1} = \frac{4}{\Delta t^2}\mathbf{q}_{n+1} + \hat{\ddot{\mathbf{q}}}_n \qquad (18)$$

$$\dot{\mathbf{p}}_{n+1} = \frac{2}{\Delta t}\mathbf{p}_{n+1} + \hat{\dot{\mathbf{p}}}_n$$

being,

$$\hat{\dot{\mathbf{q}}}_n = -\left(\frac{2}{\Delta t}\mathbf{q}_n + \dot{\mathbf{q}}_n\right)$$

$$\hat{\ddot{\mathbf{q}}}_n = -\left(\frac{4}{\Delta t^2}\mathbf{q}_n + \frac{4}{\Delta t}\dot{\mathbf{q}}_n + \ddot{\mathbf{q}}_n\right) \qquad (19)$$

$$\hat{\dot{\mathbf{p}}}_n = -\left(\frac{2}{\Delta t}\mathbf{p}_n + \dot{\mathbf{p}}_n\right)$$

that is, the pressure derivatives use the same integration scheme as do the velocities.

If dynamic equilibrium is established at time step $n+1$ by introducing the difference equations (18-19) into the differential equations (17), the following result is obtained,

$$\frac{4}{\Delta t^2}\mathbf{M}\mathbf{q}_{n+1} + \mathbf{\Phi}_{\mathbf{q}n+1}^T\left(\alpha\mathbf{\Phi}_{n+1} + \boldsymbol{\lambda}_{n+1}\right) - \mathbf{Q}_{n+1} + \mathbf{M}\hat{\ddot{\mathbf{q}}}_n = 0 \qquad (20)$$

$$\frac{2}{\Delta t}\mathbf{p}_{n+1} - \mathbf{h}_{n+1} + \hat{\dot{\mathbf{p}}}_n = 0 \qquad (21)$$

The scaling of Eq. (20-21) by a factor of $\Delta t^2/4$ is now performed, as it was done in the previous Section for the multibody problem, thus yielding

$$\mathbf{M}\mathbf{q}_{n+1} + \frac{\Delta t^2}{4}\mathbf{\Phi}_{\mathbf{q}n+1}^T\left(\alpha\mathbf{\Phi}_{n+1} + \boldsymbol{\lambda}_{n+1}\right) - \frac{\Delta t^2}{4}\mathbf{Q}_{n+1} + \frac{\Delta t^2}{4}\mathbf{M}\hat{\ddot{\mathbf{q}}}_n = 0 \qquad (22)$$

$$\frac{\Delta t}{2}\mathbf{p}_{n+1} - \frac{\Delta t^2}{4}\mathbf{h}_{n+1} + \frac{\Delta t^2}{4}\hat{\dot{\mathbf{p}}}_n = 0 \qquad (23)$$

or, symbolically $\mathbf{f}(\mathbf{x}_{n+1}) = 0$, with $\mathbf{x}^T = \left\{\begin{array}{cc} \mathbf{q}^T & \mathbf{p}^T \end{array}\right\}$.

In order to obtain the solution of this nonlinear system, the iterative Newton-Raphson method is used,

$$\left[\frac{\partial \mathbf{f}\,(\mathbf{x})}{\partial \mathbf{x}}\right]_i \Delta \mathbf{x}_{i+1} = -\,[\mathbf{f}\,(\mathbf{x})]_i \tag{24}$$

with the residual vector,

$$[\mathbf{f}\,(\mathbf{x})] = \frac{\Delta t^2}{4}\left\{\begin{array}{c}\mathbf{M}\ddot{\mathbf{q}} + \boldsymbol{\Phi}_{\mathbf{q}}^T \alpha \boldsymbol{\Phi} + \boldsymbol{\Phi}_{\mathbf{q}}^T \boldsymbol{\lambda}^* - \mathbf{Q} \\ \dot{\mathbf{p}} - \mathbf{h}\end{array}\right\} \tag{25}$$

and the approximated tangent matrix $\left[\dfrac{\partial \mathbf{f}\,(\mathbf{x})}{\partial \mathbf{x}}\right]$,

$$\left[\begin{array}{cc}\mathbf{M} + \dfrac{\Delta t}{2}\mathbf{C} + \dfrac{\Delta t^2}{4}\left(\boldsymbol{\Phi}_{\mathbf{q}}^T \alpha \boldsymbol{\Phi}_{\mathbf{q}} + \mathbf{K}\right) & -\dfrac{\Delta t^2}{4}\dfrac{\partial \mathbf{Q}}{\partial \mathbf{p}} \\[2ex] -\dfrac{\Delta t}{2}\left(\dfrac{\Delta t}{2}\dfrac{\partial \mathbf{h}}{\partial \mathbf{q}} + \dfrac{\partial \mathbf{h}}{\partial \dot{\mathbf{q}}}\right) & \dfrac{\Delta t}{2}\left(\mathbf{I}_{np} - \dfrac{\Delta t}{2}\dfrac{\partial \mathbf{h}}{\partial \mathbf{p}}\right)\end{array}\right] \tag{26}$$

Here np is the number of elements in the vector of pressures $\mathbf{p}$, and $\mathbf{I}_{np}$ is the identity matrix of such a dimension. It must be pointed out that the tangent matrix is not symmetric any more, as it was when dealing with the multibody problem alone. This fact will negatively affect the efficiency, since specific solvers for symmetric matrices are faster.

Once the Newton-Raphson iteration process converges, the resulting velocities and accelerations should be projected into their respective constraint manifolds in order to achieve constraint satisfaction at velocity and acceleration levels. The projection equations are exactly the same as those presented in Eq. (14-15).

4. The example

The example to test this approach is shown in Fig. 2. The solution obtained using the proposed formulation is compared against those obtained through other approaches. Comparison with the approach consisting of kinematically guiding the actuator will make it possible to assess the loss in efficiency incurred by the unified approach. Comparison with a co-integration scheme will allow appraising the accuracy achieved by the unified approach.

The rod, with length L=1 m and mass m=200 kg uniformly distributed, is pinned to the ground at one of its ends in A, and has attached a point mass of M=250 kg at the other end. The system is subject to gravity. A hydraulic actuator is pinned to the center point of the rod at one end, and to the ground
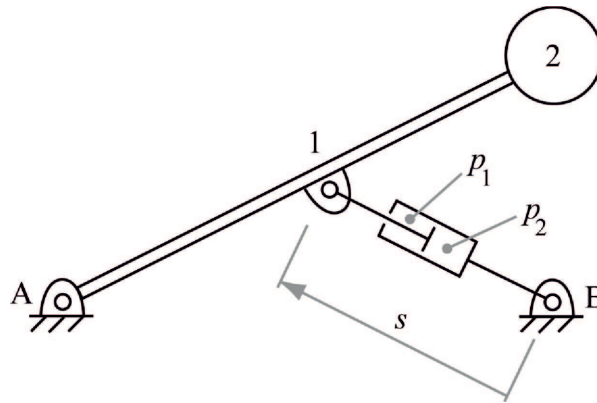
Fig. 2. The mechanism employed in the example

at the other end in B. The piston area is $A=0.0065$ m^2, and the total cylinder length is $l=0.442$ m. Friction in the actuator has been considered through a linear viscous model, with coefficient $c=10^5$ Ns/m. Coordinates of the fixed points are A(0,0) and B($\sqrt{3}/2,0$). Initially, the system is at rest, the angle between the rod and the ground is 30°, and the two cylinder chambers have the same volume.

The multibody system is modeled with the five variables grouped into vector $\mathbf{q}$, while the hydraulic actuator is modeled with the two pressures of vector $\mathbf{p}$,

$$\mathbf{q}^T = \left\{ \begin{array}{ccccc} x_1 & y_1 & x_2 & y_2 & s \end{array} \right\}$$
$$\mathbf{p}^T = \left\{ \begin{array}{cc} p_1 & p_2 \end{array} \right\} \tag{27}$$

where x_1, y_1 are the Cartesian coordinates of point 1, located in the middle of the rod, x_2, y_2 are the Cartesian coordinates of point 2, coincident with the point mass rigidly attached to the end of the rod, s is the variable length of the hydraulic actuator, and p_1, p_2 are the pressures in the upper and lower chamber of the cylinder, respectively. The meaning of all these variables is also illustrated in Fig. 2.

According to the described data, the term of the applied forces vector $\mathbf{Q}$ of Eq. (17) due to the hydraulic actuator is,

$$\mathbf{Q}(5) = (p_2 - p_1)A - c\dot{s} \tag{28}$$

Regarding the second set of equations in Eq. (17), i.e. the pressure equations, they are stated as follows,

$$\dot{p}_1 = h_1 = \frac{\beta_1}{Al_1}\left[A\dot{s} + A_i c_d \sqrt{\frac{2(p_P - p_1)}{\rho}}\delta_P - A_o c_d \sqrt{\frac{2(p_1 - p_T)}{\rho}}\delta_T\right]$$
$$\dot{p}_2 = h_2 = \frac{\beta_2}{Al_2}\left[-A\dot{s} + A_o c_d \sqrt{\frac{2(p_P - p_2)}{\rho}}\delta_P - A_i c_d \sqrt{\frac{2(p_2 - p_T)}{\rho}}\delta_T\right] \tag{29}$$

where β_i is calculated according to Eq. (3), l_1 and l_2 are the variable lengths of the upper and lower chamber, respectively, A_i and A_o are the variable valve areas connecting the cylinder chambers to the pump and to the tank, respectively, $c_d=0.67$ is the valve discharge coefficient, $\rho=850$ kg/m^3 is the fluid density, $p_P=7.6$ MPa and $p_T=0.1$ MPa are the pump and tank pressures, respectively (considered constant in this example), and, finally, δ_P and δ_T are 0 in case the quantity inside the square root is negative, and 1 otherwise.

Given that the two cylinder chambers have equal volume at initial time, the variable lengths of the upper and lower chamber are obtained as,

$$l_1 = 0.5l + s_o - s$$
$$l_2 = 0.5l + s - s_o \tag{30}$$

with $s_o=0.5$ m the initial length of the actuator.

The variable valve areas A_i and A_o take, for each time instant, the following values,

$$A_i = 0.0005\kappa$$
$$A_o = 0.0005(1 - \kappa) \tag{31}$$

where κ is the spool displacement or valve control parameter, i.e. the input which controls the system motion.

The initial values of the problem variables are set so that the system is in static equilibrium. This serves to avoid instabilities in the integration process. The values of the position variables, $\mathbf{q}$, are easily obtained from the initial configuration of the system described above. The initial velocities, $\dot{\mathbf{q}}$, are set to zero, since the system is at rest. The initial values of the pressures, $\mathbf{p}$, are calculated as the solution of a nonlinear system formed by the three following equations:

$$(2M + m)g = (p_2 - p_1)A$$
$$h_1 = 0 \tag{32}$$
$$h_2 = 0$$

where g=9.81 m/s^2 is the value of gravity. The solution of the nonlinear system of Eq. (32) yields the initial values of the pressures p_1 and p_2 and the initial value of the spool displacement κ, so that static equilibrium is guaranteed.

In order to build the combined dynamic equations provided in Eq. (17), some additional terms are required.

The mass matrix is,

$$\mathbf{M} = \begin{bmatrix} 0 & 0 & 0 & 0 & 0 \\ 0 & 0 & 0 & 0 & 0 \\ 0 & 0 & M + \dfrac{m}{3} & 0 & 0 \\ 0 & 0 & 0 & M + \dfrac{m}{3} & 0 \\ 0 & 0 & 0 & 0 & 0 \end{bmatrix} \tag{33}$$

The inertia of the rod has been distributed between point A (fixed) and point 2, so that no inertia has been assigned to point 1, thus yielding the null first and second rows and columns of the mass matrix.

The applied forces are,

$$\mathbf{Q} = \begin{Bmatrix} 0 \\ -mg \\ 0 \\ -Mg \\ (p_2 - p_1)A - c\dot{s} \end{Bmatrix} \tag{34}$$

and the constraints vector is,

$$\Phi = \begin{Bmatrix} (x_1 - x_A)^2 + (y_1 - y_A)^2 - (0.5L)^2 \\ (x_2 - x_A) - 2(x_1 - x_A) \\ (y_2 - y_A) - 2(y_1 - y_A) \\ (x_1 - x_B)^2 + (y_1 - y_B)^2 - s^2 \end{Bmatrix} \tag{35}$$

where the first equation imposes the constant length of segment $\overline{A1}$, the second and third equations indicate that vector $\overline{A2}$ is proportional to vector $\overline{A1}$, and the fourth equation relates the variable actuator distance s with the Cartesian coordinates of points 1 and B.

Finally, in order to build the approximate tangent matrix of Eq. (26), the following terms are also required. The stiffness matrix $\mathbf{K}$ is null in this example, while the damping matrix $\mathbf{C}$ has only one non-zero element due to the viscous damping at the actuator, $\mathbf{C}(5,5)=c$. Moreover,

$$
\frac{\partial \mathbf{Q}}{\partial \mathbf{p}} = A \begin{bmatrix} 0 & 0 \\ 0 & 0 \\ 0 & 0 \\ 0 & 0 \\ -1 & 1 \end{bmatrix}
$$

$$
\frac{\partial \mathbf{h}}{\partial \mathbf{q}} = \begin{bmatrix} 0 & 0 & 0 & 0 & \dfrac{h_1}{l_1} \\ 0 & 0 & 0 & 0 & -\dfrac{h_2}{l_2} \end{bmatrix} \tag{36}
$$

$$
\frac{\partial \mathbf{h}}{\partial \dot{\mathbf{q}}} = \begin{bmatrix} 0 & 0 & 0 & 0 & \dfrac{\beta}{l_1} \\ 0 & 0 & 0 & 0 & -\dfrac{\beta}{l_2} \end{bmatrix}
$$

$$
\frac{\partial \mathbf{h}}{\partial \mathbf{p}} = -\frac{\beta c_d}{A \sqrt{2\rho}} \begin{bmatrix} D & 0 \\ 0 & E \end{bmatrix}
$$

where D and E are obtained as,

$$
\begin{aligned}
D &= \frac{1}{l_1} \left(\frac{A_i}{\sqrt{p_P - p_1}} \delta_P + \frac{A_o}{\sqrt{p_1 - p_T}} \delta_T \right) \\
E &= \frac{1}{l_2} \left(\frac{A_o}{\sqrt{p_P - p_2}} \delta_P + \frac{A_i}{\sqrt{p_2 - p_T}} \delta_T \right)
\end{aligned} \tag{37}
$$

A 10-seconds analysis is defined as the case-study: starting from rest initial conditions, the spool displacement κ is varied according to the following law:

$$
\kappa = \begin{cases} \kappa_o & t \leqslant 2 \\ \kappa_o - 0.01 & 2 < t \leqslant 6 \\ \kappa_o + 0.01 & 6 < t \leqslant 10 \end{cases} \tag{38}
$$

where κ_o is the initial value of the control parameter, which provides static equilibrium conditions, as explained before. The areas of the orifices depend on the displacement of the spool according to Eq. (31).

Chronologically, the proposed unified scheme was first run and the histories of the cylinder length s and its first and second time-derivatives were stored during the simulation.

In the second simulation executed, a program which implements the simplified approach (kinematic guidance of the actuator) was run. The histories

of the cylinder length and its derivatives, stored in the previous simulation, were recovered and used to kinematically guide the coordinate *s* of the multibody problem, so that the same motion of the system was ensured. It must be pointed out that this second simulation is not a kinematic simulation, but a dynamic one provided by the formalism described in Section 2, in which the value of the problem variable associated to the cylinder, *s*, is imposed by means of an additional kinematic constraint (in the general case, knowing the motion of the hydraulic cylinders does not imply that the full system motion is known and, hence, the equations of motion should still be integrated). Therefore, the constraints vector is not that shown in Eq. (35), but the following one,

$$\Phi = \left\{ \begin{array}{c} (x_1 - x_A)^2 + (y_1 - y_A)^2 - (0.5L)^2 \\ (x_2 - x_A) - 2(x_1 - x_A) \\ (y_2 - y_A) - 2(y_1 - y_A) \\ (x_1 - x_B)^2 + (y_1 - y_B)^2 - s^2 \\ s - s(t) \end{array} \right\} \tag{39}$$

Finally, a third simulation implementing a multi-rate integration scheme (different integrators and time steps) was carried out. The multibody problem conducted the integration. A time step of 10 ms was adopted for the multibody integration, while the hydraulic problem was integrated through a forward Euler integrator with a time step of 0.2 ms, the largest that reached convergence. These time-step sizes imply that, at every iteration of the multibody problem, the hydraulic problem must be integrated 50 times.

The integration of the hydraulic expressions given in Eq. (29) assumes a constant elongation velocity of the actuator during the multibody time step. This velocity is approximated by the length variation divided by the time-step size:

$$\dot{s} = \frac{s(t_{n+1}) - s(t_n)}{\Delta t} \tag{40}$$

The Newton-Raphson scheme of the multibody integration yields, at every iteration step, a variation of the elongation at time t_{n+1}, so that a new integration of the hydraulic equations is required. Therefore, the total time of the simulation will be larger than in the case of the unified approach. However, the theoretically more accurate solution will serve to validate the solution provided by the scheme proposed in this paper.

The results obtained from the three simulations, along with their discussion, are addressed in the next Section.

5. Results and discussion

Fig. 3 shows the histories of the cylinder length, s, and its first derivative, $\dot{s}$. Fig. 4 plots the difference between the elongation, s, obtained by the unified method and the multi-rate integration. Fig. 5 presents the histories of the pressures p_1 and p_2. A detail of the discrepancies between both solutions is presented in Fig. 6, where the grey line provides the solutions of the multi-rate integration while the black line represents the solutions of the unified method.

Fig. 7 illustrates the actuator force, including the damping losses. Fig. 8 plots the histories of the total energy, the kinetic energy, the potential energy, and the work performed by the actuator (including the damping losses again). Fig. 9 displays the violation of the constraints and their first and second derivatives (in all the three cases, the plotted magnitude is the norm of the corresponding vector). The abrupt jumps at $t = 2$ s and $t = 6$ s are due to the sudden changes of the spool motion at those instants. At $t = 2$ s the mechanism is in equilibrium position, so that the influence of starting the spool motion is lower than that of stopping it at $t=6$ s. The constraints behavior reveals the difficulty of keeping the mechanism assembled under the actuating forces. Anyway, the norm of the constraints vector is kept under the imposed tolerance of 1.e-7.

Solutions in position, velocity and acceleration of the cylinder show practically no discrepancies between the two methods. Because of this, only one single line can be seen in the plots and the difference between the solution provided by the multi-rate and unified integration is detailed in Fig. 4. Notice that this difference is under 0.1 mm in the positions.

In order to validate the solution of the unified scheme, a comparison of the evolution of the pressures is illustrated in Fig. 5 and a detail of the pick value of pressure p_1 is provided in Fig. 6. As explained before, the hydraulic problem is stiff, this behavior being evidenced in Fig. 6. The multi-rate scheme employs a smaller integration step for the hydraulic problem and therefore yields a smoother solution. In general terms, the solution of the unified scheme is accurate and oscillations are not relevant.

It must be said that, although typical values of the penalty factor α (see Eq. (5)) are in the range 10^7-10^9, in this case a value of $\alpha=10^{10}$ has been shown to provide the best convergence properties for the Newton-Raphson iteration of the unified scheme. The need of such a large penalty factor is due to the stiffness introduced in the system by the hydraulic equations.
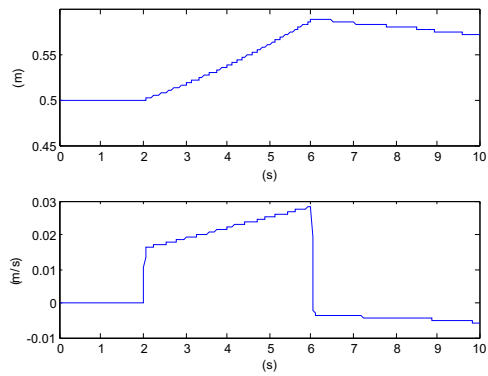
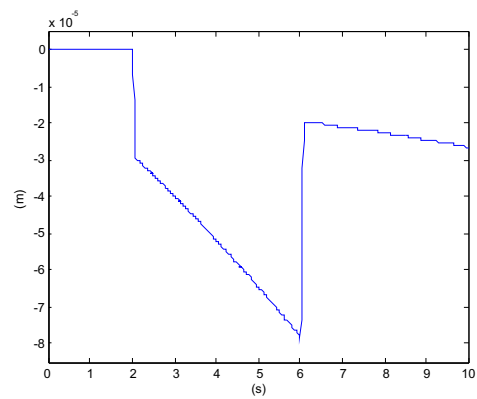Fig. 3. Histories of the cylinder length, s, and its first derivative, $\dot{s}$

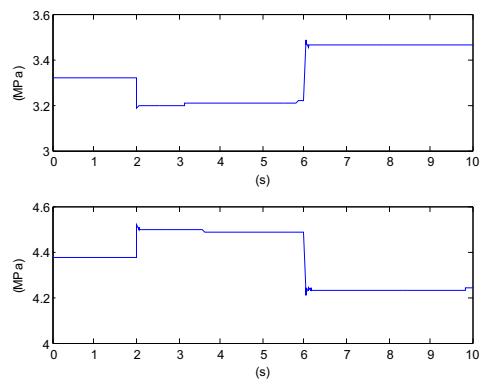Fig. 4. Difference between the histories of the cylinder elongation obtained by multi-rate and unified method

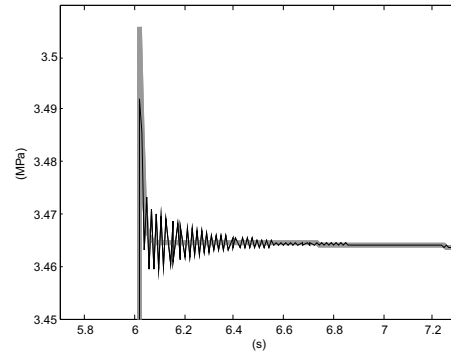Fig. 5. Histories of the pressures p_1 and p_2

Fig. 6. Detail of the discrepancies between p_1 values obtained by multi-rate (grey) and unified method (black)
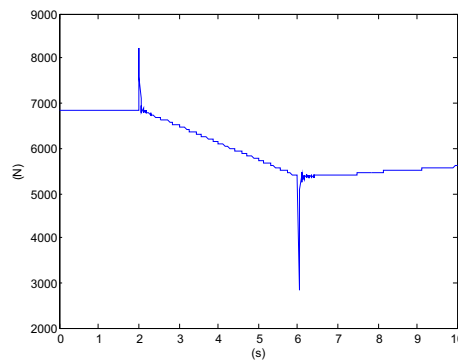

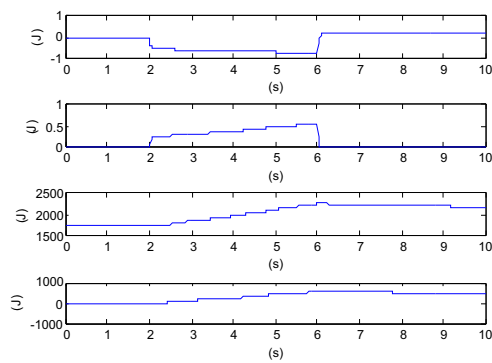Fig. 7. History of the actuator force, including the damping losses

Fig. 8. Histories of the total, kinetic and potential energy, and actuator work
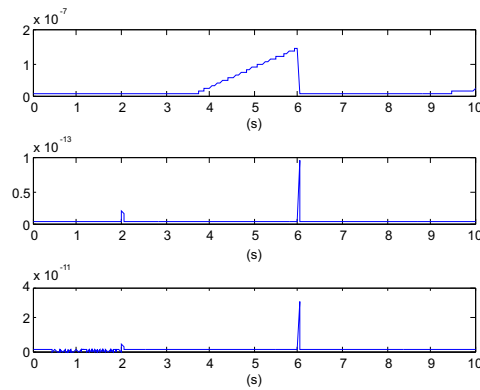
Fig. 9. Violation of the constraints and their first and second derivatives

In regard to the integration time-step size, the plotted results in Figs. 3 through 9 have been obtained with a fixed time-step of 10 ms for the unified integration scheme, the multibody part of the multi-rate integration scheme, and the simplified simulation. Of course, smaller time-step sizes have been tested too and can be used without any problem. The integration time-step size for the hydraulic problem in the multi-scale scheme has been set to 0.2 ms. Larger time steps did not reach convergence when using the forward Euler integrator. However, if the trapezoidal rule is employed, a time-step size of 10 ms can be reached. In this case, the histories of the pressures are equal to those obtained with the unified scheme and showed in Fig. 5.

The number of iterations required for convergence with $\alpha=10^{10}$ and $\Delta t=10$ ms has been two or three at the more demanding instants of the simulation (around $t=2$ s and $t=6$ s) and just one for the rest. The plot of the total energy in Fig. 6 shows good conservation properties: there is a variation of 1 J in the total energy during the simulation, which is a small quantity compared to variations of potential energy and actuator work of around 1000 J. The plots of constraints violation at position, velocity and acceleration levels in Fig. 7 prove that constraint satisfaction is kept within very strict limits. Therefore, the algorithm has shown a good behavior for such a large time-step size of integration, which confirms that it conserves the robustness already demonstrated in multibody simulations.

Regarding the efficiency, CPU-times measured for the three simulations performed are shown in Table 1. The programs were developed and run in Matlab computing environment, which means that absolute CPU-times are not representative, yet they serve for comparison among the different approaches.

In Table 1, the increase in computational cost motivated by the inclusion of the hydraulic equations in the unified scheme is around 20% with respect to the simplified simulation, that only considers the multibody problem. From a theoretical point of view, the increase in computational cost is basically due to two factors: first, to the larger problem size, since the pressures are added to the problem variables, and, second, to the non-symmetric character of the new approximated tangent matrix of the Newton-Raphson iteration.

Table 1.

CPU-times for the three compared approaches

Simulation		CPU-time (s)
Kinematic guidance		0.338
Unified integration		0.389
Multi-rate integration	Forward Euler (Δt = 0.2 ms)	5.895
	Trapezoidal Rule (Δt = 10 ms)	0.672

The comparison between the unified scheme and the multi-rate approach is very favorable to the unified scheme. Multi-rate integration with the forward Euler integrator implies to evaluate and integrate the hydraulic equations 50 times at each iteration within a time step of the multibody integration. As can be seen in Table 1, the use of a more stable integrator as the trapezoidal rule for the hydraulic problem leads to a smaller difference between the unified and multi-rate schemes, since this integrator allows to employ a time-step size of 10 ms for the integration of the hydraulic problem.

Table 2 shows the fastest simulations that provide a smooth solution of the pressure problem when a multi-rate integration is performed. As it can be seen, the simulation does not converge for time-step sizes larger than 0.2 ms with the forward Euler integrator. In the case of the trapezoidal rule, a time-step size of 5 ms can be reached; faster simulations are also possible, but larger time-step sizes lead to non-smooth results.

Table 2.

Fastest simulations with smooth solution of the hydraulic problem for multi-rate integration

Integrator	CPU-time (s)
Forward Euler (Δt = 0.2 ms)	5.895
Trapezoidal Rule (Δt = 5 ms)	1.021

Finally, Table 3 shows the main features of the different approaches. When considering the kinematic guidance, precision is not taken into account because the actual hydraulic problem is not resolved. Regarding the multi-rate integration with the trapezoidal rule as integrator for the hydraulic problem,

the presented characteristics correspond to a time-step size of 5 ms, since this is the largest one that provides a smooth solution.

Table 3.

Properties of the different methods

Simulation		Efficiency	Accuracy	Ease of implement.
Kinematic guidance		*****	–	*****
Unified integration		*****	***	*
Multi-rate integration	Forward Euler	*	*****	****
	Trapezoidal Rule	***	*****	****

Several consequences can be derived from Table 3. The use of the unified integration scheme is adequate when efficiency is paramount. Otherwise, the multi-rate integration is recommended; in such a case, the use of the trapezoidal rule as integrator provides a good compromise between efficiency and accuracy.

Evidently, these trends require further confirmation in the simulation of large and complex machines like, for example, the full model of an excavator, but the analysts interested in moving from the simplified approach to the integration of the hydraulic equations may use this study as a starting point.

6. Conclusions

Based on the results reported herein, the following conclusions can be established:

- The augmented Lagrangian formulation traditionally used to address multi-body dynamics problems preserves its robustness when facing combined multibody and hydraulic dynamics problems in a unified approach. For the academic example studied, a large time-step size of 10 ms could be taken, but a high penalty factor of 10^{10} was required in order to keep good convergence properties, due to the stiffness of the hydraulic equations.
- The increase in computational cost motivated by the inclusion of the hydraulic equations when compared with a simplified modeling of the hydraulic problem through kinematic guidance of the actuators is moderated, and due mainly to the larger resulting problem size and the non-symmetric character of the approximated tangent matrix. A 20% increase

was measured for the academic example considered. Therefore, it can be affirmed that efficiency is not substantially altered when moving from a simplified to a fully-coupled approach.

- The unified approach is more efficient than the multi-rate integration scheme due to the lower number of evaluations of the hydraulic equations required. However, this higher efficiency is achieved at the cost of obtaining a less smooth solution for the hydraulics.
- If a smooth solution of the hydraulics is required, the multi-rate integration scheme with an implicit integrator for the hydraulic problem provides a good compromise between efficiency and accuracy, and requires less implementation effort than the unified approach.

REFERENCES

[1] Cuadrado J., Cardenal J., Morer P., Bayo E.: Intelligent Simulation of Multibody Dynamics: Space-State and Descriptor Methods in Sequential and Parallel Computing Environments, *Multibody System Dynamics*, Vol. 4, pp. 55-73, 2000.
[2] Cuadrado J., Dopico D., Gonzalez M., Naya M.A.: A Combined Penalty and Recursive Real-Time Formulation for Multibody Dynamics, *Journal of Mechanical Design*, Vol. 126, pp. 602-608, 2004.
[3] Fales R., Spencer E., Chipperfield K., Wagner F., Kelkar A.: Modeling and Control of a Wheel Loader with a Human-in-the-Loop Assessment using Virtual Reality, *Journal of Dynamic Systems, Measurement, and Control*, Vol. 127, pp. 415-423, 2005.
[4] Sekhavat P., Sepehri N., Wu Q.: Impact Stabilizing Controller for Hydraulic Actuators with Friction: Theory and Experiments, *Control Engineering Practice*, Vol. 14, pp. 1423-1433, 2005.
[5] Merritt H.E.: *Hydraulic Control Systems*, Wiley, New York, 1967.
[6] Eryilmaz B., Wilson B.H.: Unified Modeling and Analysis of a Proportional Valve, *Journal of the Franklin Institute*, Vol. 343, pp. 48-68, 2006.
[7] Gonzalez M., Luaces A., Dopico D., Cuadrado J.: A 3D Physics-Based Hydraulic Excavator Simulator, *Proceedings of the ASME World Conference on Innovative Virtual Reality (WINVR09)*, Paper 734, Chalon-sur-Saone, France, 2009.
[8] Vaculin M., Valasek M., Krüger W.R.: Overview of Coupling of Multibody and Control Engineering Tools, *Vehicle System Dynamics*, Vol. 41, pp. 415-429, 2004.
[9] Valasek M.: Modeling, Simulation and Control of Mechatronical Systems, *Simulation Techniques for Applied Dynamics (Arnold M. and Schiehlen W. eds.)*, Springer, Wien-New York, 2008.
[10] Brüls O., Arnold M.: The Generalized-α Scheme as a Linear Multistep Integrator: Towards a General Mechatronic Simulator, *Proceedings of the ASME Int. DETC & CIEC*, Las Vegas, Nevada, USA, 2007.

[11] Pfeiffer F., Foerg M., and Ulbrich H.: Numerical Aspects of Non-Smooth Multibody Dynamics. *Computer Methods in Applied Mechanics and Engineering*, Vol. 195, pp. 6891-6908, 2006.

[12] Busch M., Arnold M., Heckmann A., Dronka S.: Interfacing SIMPACK to Modelica/Dymola for Multi-Domain Vehicle System Simulations, *SIMPACK News*, Vol. 11, No. 2, pp. 1-3, 2007.

[13] Cardona A. and Geradin M.: Modeling of a Hydraulic Actuator in Flexible Machine Dynamics Simulation, *Mechanisms and Machine Theory*, Vol. 25, pp. 193-207, 1990.

[14] Bauchau O.A. and Liu H.: On the Modeling of Hydraulic Components in Rotorcraft Systems, *Journal of the American Helicopter Society*, Vol. 51, pp. 175-184, 2006.

[15] Welsh W.A.: Simulation and Correlation of a Helicopter Air-Oil Strut Dynamic Response, *Proceedings of the American Helicopter Society 43rd Annual Forum*, St. Louis, Missouri, USA, 1987.

[16] Garcia de Jalon J., Bayo E.: *Kinematic and Dynamic Simulation of Multibody Systems –The Real-Time Challenge–*, Springer-Verlag, New York, 1994.

Skuteczna, zunifikowana metoda połączonej symulacji dynamiki systemu wieloczłonowego i hydraulicznego: porównanie podejścia uproszczonego i integracyjnego

S t r e s z c z e n i e

W Laboratorium Budowy Maszyn (Laboratory of Mechanical Engineering) Uniwersytetu La Coruña opracowano solidne i skuteczne sformułowanie problemu symulacji umożliwiające symulację dużych, skomplikowanych systemów wieloczłonowych. Opracowano symulatory samochodów, koparek i innych maszyn wykazując, że można wykonać symulacje w czasie rzeczywistym, nawet w sytuacji skomplikowanych manewrów.

Siłowniki hydrauliczne są wykorzystywane w wielu zastosowaniach przemysłowych w systemach wieloczłonowych, np. w maszynach roboczych. Przy symulacji tego rodzaju systemów, w których występuje połączenie hydrauliki z dynamiką systemów wieloczłonowych, można najczęściej zastosować jedno z dwu podejść: ograniczyć się do kinematycznego sterowania zmienną długością siłownika, unikając w ten sposób konieczności uwzględnienia dynamiki systemu hydraulicznego albo, gdy wymagany jest bardziej szczegółowy opis problemu, np. gdy celem symulacji jest optymalizacja sterowania pompy, wykonać wielostopniowe całkowanie w obydwu systemach.

W przedstawionej pracy dokonano włączenia dynamiki siłowników hydraulicznych do wspomnianego wyżej samodzielnego sformułowania dla systemu wieloczłonowego, co doprowadziło do podejścia zunifikowanego. Zaprezentowano przykład akademicki, w którym porównano efektywność, dokładność i łatwość implementacji podejść uproszczonego (sterowanie kinematyczne), wielostopniowego i zunifikowanego. To porównanie jest najważniejszym przyczynkiem, jaki wnosi prezentowana praca, gdyż może służyć wskazaniu wyboru właściwego podejścia w zależności od charakterystyk problemu.